RESEARCH ARTICLE

Editorial Process: Submission:12/29/2025 Acceptance:02/25/2026 Published:07/27/2026

Arginase 2 Downregulation in High-Grade Prostate Adenocarcinoma and Its Spatial Inverse Association with Tumor-Infiltrating Lymphocytes

Arif Budiman Kaharuddin[1], Muhammad Husni Cangara[1,2]*, Upik A Miskad[1,2], Syarifuddin Wahid[2,3], Djumadi Achmad[2,3], Berti Julian Nelwan[1,2,3]

Abstract

Objective: The interaction between metabolic enzymes and the immune microenvironment in prostate cancer is still complex. This study aimed to examine the relationship between *Arginase 2* (*ARG2*) expression and tumor-infiltrating lymphocytes (TILs) in prostate adenocarcinoma patients, as well as its correlation with histopathological grading, thereby elucidating immunometabolic mechanisms within the Indonesian patient population. **Methods:** This observational analytic study utilized a cross-sectional design, incorporating 105 formalin-fixed paraffin-embedded (FFPE) tissue blocks of prostate adenocarcinoma obtained from referral hospitals in Makassar, Indonesia. Immunohistochemistry was used to find out how much *ARG2* was expressed, and digital image analysis (QuPath) was used to get an objective H-Score. According to the International Immuno-Oncology Biomarkers Working Group guidelines, the density of TILs was measured on H&E-stained slides. Statistical analyses encompassed Spearman's rank correlation, the Kruskal-Wallis test, and the Wilcoxon Signed-Rank test for spatial analysis. **Result:** The study population was predominantly characterized by high-grade tumors, with 45.7% categorized as Grade Group V (Gleason Score 9–10). The digital quantification of *ARG2* was validated by manual scoring ($r = 0.768$, $p < 0.001$). There was no statistically significant correlation between *ARG2* expression and TILs density on a global scale ($r = 0.048$, $p = 0.630$). Nonetheless, paired spatial analysis indicated a significant local disparity; tumor regions infiltrated by TILs demonstrated substantially diminished *ARG2* expression relative to adjacent non-infiltrated regions ($p = 0.009$). Moreover, *ARG2* expression exhibited a significant inverse correlation with WHO Grade Group ($p < 0.001$), indicating substantial downregulation in high-grade tumors. **Conclusion:** The expression of *Arginase 2* is significantly reduced in high-grade prostate adenocarcinoma, signifying tumor dedifferentiation. Although *ARG2* does not universally forecast immune infiltration, it influences the tumor microenvironment locally, with increased expression correlating with immune exclusion.

Keywords: Prostate Adenocarcinoma - *Arginase 2* - Tumor-Infiltrating Lymphocytes - Digital Pathology

Asian Pac J Cancer Prev, **27 (7)**, 2713-2719

Introduction

Prostate cancer is a big health problem for men all over the world. The Global Cancer Observatory's 2022 data shows that prostate cancer is very common around the world, with 1,466,680 diagnosed cases and 396,792 deaths [1]. Although the incidence in Indonesia is still lower than in Western countries, it has been steadily rising over the past few decades [2]. In developed nations, early detection typically reveals localized cases; however, around 50% of prostate cancer patients in Indonesia exhibit metastatic disease, resulting in a worse prognosis and significant economic burdens [3–5].

The advancement of prostate cancer is influenced by both the characteristics of tumor cells and intricate interactions within the tumor microenvironment (TME), encompassing metabolic changes and immune responses [6]. Arginase, an essential metabolic enzyme in carcinogenesis, is present in two isoforms: cytosolic Arginase 1 (ARG1) and mitochondrial *Arginase 2* (*ARG2*). *Arginase 2* is abundantly expressed in normal prostate tissue and is essential for the conversion of L-arginine into L-ornithine and urea [7]. In the context of cancer, it is hypothesized that *ARG2* dysregulation affects the availability of arginine, which is crucial for cell proliferation and immune function [8].

The precise function of *ARG2* in the tumorigenesis of prostate cancer is still under discussion. Certain

*[1]Department of Anatomical Pathology, Faculty of Medicine, Hasanuddin University, Indonesia. [2]Anatomical Pathology Laboratory, Hasanuddin University Hospital, Indonesia. [3]Sentra Diagnostik Patologia Makassar, Makassar, Indonesia. *For Correspondence: husnicangara@med.unhas.ac.id*

studies indicate that arginase facilitates tumorigenesis by supplying polyamines essential for cellular proliferation [7, 9]. On the other hand, some studies suggest that high levels of *ARG2* may stop prostate cancer cells from growing, moving, and invading, which could make it a good sign for the future [10]. But a very important part of *ARG2*'s activity is that it can make the immune system less effective. The enzyme can stop Tumor-Infiltrating Lymphocytes (TILs) from growing and activating by depleting extracellular L-arginine. This is especially true for CD8+ T cells, which need arginine a lot to do their cytotoxic functions [10, 11].

Tumor-Infiltrating Lymphocytes (TILs) are known to be important prognostic factors in many types of cancer. A high number of TILs is often linked to better clinical outcomes, which shows that the immune system is actively fighting the tumor [12]. Nonetheless, the precise mechanism by which *ARG2* regulates TIL density and activity in prostate adenocarcinoma remains inadequately elucidated. Current hypotheses suggest that elevated *ARG2* expression results in diminished TIL infiltration, culminating in an immunologically "cold" tumor phenotype [13, 14]. This study aims to investigate the correlation between *Arginase 2* expression and tumor-infiltrating lymphocytes in prostate adenocarcinoma patients, along with its association with histopathological grading, to offer novel insights into immuno-metabolic mechanisms within the Indonesian patient demographic.

Materials and Methods

Study Design and Participants

This observational analytic study utilized a cross-sectional design and was conducted at the Anatomical Pathology Laboratory, Faculty of Medicine, Hasanuddin University, Makassar, from August to December 2025. The study population consisted of formalin-fixed paraffin-embedded (FFPE) tissue blocks of prostate adenocarcinoma obtained from Dr. Wahidin Sudirohusodo Hospital, Hasanuddin University Hospital, and Sentra Diagnostik Patologia Makassar.

Samples were chosen through a total sampling method, utilizing the admission sequence of tissues, with a retrospective timeline extending from September 2025. The inclusion criteria consisted of tissue blocks from radical prostatectomy, TURP, or other biopsies, histopathologically identified as prostate adenocarcinoma. Samples lacking complete clinical data (notably age), exhibiting damaged blocks, fungal contamination, or inadequate tumor tissue (<5%) were excluded. The minimum number of samples needed for the study was 84, but 105 were used in the final analysis.

Histopathology and Immunohistochemistry

Tissue blocks were sliced into pieces that were 3 µm thick. Histopathological confirmation and Gleason grading were done with Hematoxylin and Eosin (H&E) staining. For immunohistochemistry (IHC), sections were deparaffinized in xylene and then rehydrated with alcohols of different strengths. Slides were heated in a Tissue Retrieval Solution (TRS) in a microwave for 10 minutes to get the antigens back.

To reduce non-specific staining, sections were treated with peroxide for 15 minutes and protein for 5 minutes. After that, the slides were put in an incubator with the main antibody against *Arginase 2*. Ultratek anti-polyvalent (ScyTek) and then Ultratek HRP (ScyTek) were used as the detection systems. Each was incubated for 10 minutes. Diaminobenzidine (DAB) chromogen was used to make the image visible. It was then counterstained with hematoxylin, dehydrated, cleared in xylene, and mounted.

Digital Image Analysis (Arginase 2 Expression)

We used digital image analysis to measure how much *Arginase 2* was present. QuPath software (version 0.6.0) was used to analyze taken pictures of "hotspot" areas at 100x magnification. Color deconvolution was used in the pre-processing step to separate the hematoxylin and DAB staining. The Cell Detection algorithm was used to separate tumor cells from stroma. DAB intensity was used to sort cells into four groups: Negative (0), Weak (1+), Moderate (2+), and Strong (3+). We used the formula H-Score = (1 X %weak) + (2 X %moderate) + (3 X %strong) to find the Histoscore (H-Score), which ranges from 0 to 300. Two consultant pathologists confirmed that the digital analysis was correct.

Assessment of Tumor-Infiltrating Lymphocytes (TILs)

The International Immuno-Oncology Biomarkers Working Group's [15] rules were used to measure the density of tumor-infiltrating lymphocytes (TILs) on H&E-stained slides. The assessment was limited to stromal tumor-infiltrating lymphocytes located within the invasive margin and central tumor, omitting regions of necrosis, artifacts, or granulocytic infiltration. The outcome was quantified as the percentage of stromal regions infiltrated by mononuclear inflammatory cells.

Statistical Analysis

We used SPSS software to look at the statistical analysis data. We used the Shapiro-Wilk or Kolmogorov-Smirnov test to see if the data distribution was normal. The Spearman Rank Correlation test was used for bivariate analysis to look at the link between *Arginase 2* H-Scores and TILs density and to check the digital method against manual scoring. The Kruskal-Wallis test was used to compare the Grade Groups, and then the Mann-Whitney U test was used for post-hoc analysis. The Wilcoxon Signed-Rank test was used to do a spatial analysis that compared *Arginase 2* expressions in TILs areas inside tumors to those outside of tumors. A p-value of less than 0.05 was deemed statistically significant.

Results

Clinicopathologic Characteristics of the Study Population

The study population comprised 105 prostate adenocarcinoma tissue samples. The average age of patients was 70.93 years, with a range of 45 to 92 years. Most of the patients (72.4%) were older than 65 years old. Histopathologically, the cohort was characterized by high-grade tumors; 45.7% of cases were classified as Grade

Group V (Gleason Score 9–10), signifying a significant prevalence of aggressive disease within this population. On the other hand, Grade Group I (Gleason Score 6) made up 21.9% of the cases. Table 1 shows a summary of the detailed characteristics.

Validation of Digital Image Analysis

To guarantee the precision of the automated quantification, we initially validated the digital H-Scores produced by QuPath against the manual semiquantitative scores supplied by the pathologists. There was a strong positive correlation between the digital and manual methods for both the dominant Gleason pattern ($r = 0.768$, $p < 0.001$) and the secondary pattern ($r = 0.659$, $p < 0.001$). These findings validate that digital image analysis is an effective technique for quantifying *Arginase 2* expression in this research.

Expression of Arginase 2 and Tumor-Infiltrating Lymphocytes

Arginase 2 expression exhibited significant variability among samples. The average digital H-Score was 124.65 ± 63.62, with a range of 3.65 to 251.63. Most cases were classified as having weak (33.3%) or moderate (33.3%) expression by manual assessment, and 7.6% were negative (Figure 1). In terms of the immune microenvironment, the density of stromal Tumor-Infiltrating Lymphocytes (TILs) was typically low to moderate. The average percentage of TILs was 8.29% ± 10.96% (the middle value was 10.0%). Most of the samples were found to have either moderate (10–49%) infiltration (50.5%) or negligible (0–9%) infiltration (48.6%). Only one sample showed severe immune infiltration (≥50%).

Association Between Arginase 2 Expression and TILs

Our primary analysis sought to ascertain whether *Arginase 2* expression correlates with the overall density of immune infiltration. Spearman rank correlation analysis indicated no statistically significant association between *Arginase 2* H-Scores and the percentage of TILs ($r = 0.048$, $p = 0.630$). Additional subgroup analyses predicated on Gleason patterns (Dominant vs. Secondary) or the exclusion of samples exhibiting 0% TILs also did not reveal any significant correlation (Table 2).

A paired spatial analysis comparing different areas within the same tumor section, however, showed a big difference in one area. We discovered that tumor regions infiltrated by TILs (intra-tumoral TILs) exhibited markedly reduced *Arginase 2* expression relative to adjacent tumor regions devoid of TILs ($Z = -2.625$, $p = 0.009$) (Figure 2). This indicates a localized downregulation of *Arginase 2* within the specific microenvironment inhabited by immune cells.

Correlation with Histopathological Grade

We investigated how these biomarkers were related to how aggressive the tumor was by looking at how they were related to histopathological grades. A substantial inverse correlation was identified between *Arginase 2* expression and the WHO Grade Group ($p < 0.001$). The expression levels of *Arginase 2* were highest in low-grade tumors (Grade Group I; Mean Rank 74.48) and significantly decreased in high-grade tumors (Grade Group V; Mean Rank 43.67). Post-hoc analysis validated that *Arginase 2* expression in Grade Group I was markedly elevated compared to Grade Group V ($p < 0.001$), signifying that the reduction of *Arginase 2* expression correlates with tumor dedifferentiation. Conversely, no significant variation in TILs density was detected among the various Grade Groups ($p = 0.168$).

Discussion

This study sought to clarify the relationship between *Arginase 2* (*ARG2*) expression and the immune microenvironment in prostate adenocarcinoma. Our results indicate a multifaceted relationship in which *ARG2* functions as a dynamic metabolic checkpoint. The most important finding is that *ARG2* is turned down in high-grade tumors and that it has a localized inverse relationship with Tumor-Infiltrating Lymphocytes (TILs), even though there is no global correlation.

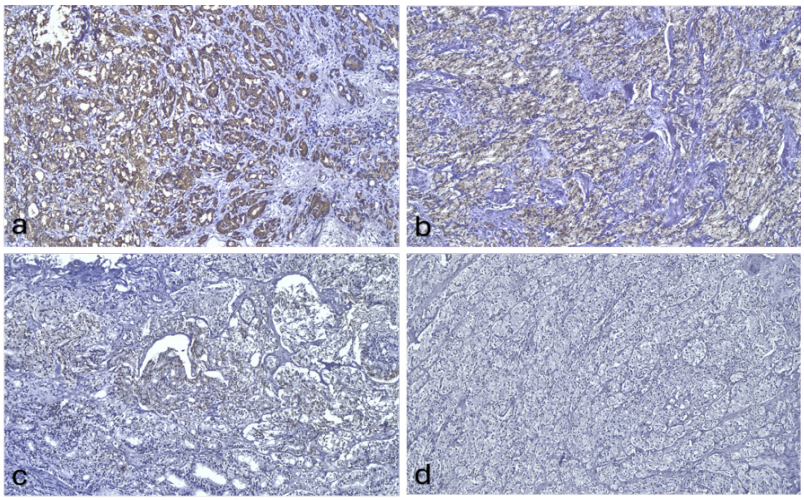

Figure 1. Representative Images of Arginase 2 Expression Intensity in Prostate Adenocarcinoma Tissue Sections. (a) Strong expression (Score +3). (b) Moderate expression (Score +2). (c) Weak expression (Score +1). (d) Negative expression (Score 0). (Immunohistochemical staining, 100x magnification).

Table 1. Clinicopathological Characteristics of Prostate Adenocarcinoma Patients (n=105)

Variable	Category / Parameter	n (%)	Mean ± SD / Median (Range)
Age (years)	Mean ± SD		70.93 ± 10.10
	Median (Min - Max)		71.0 (45 - 92)
	< 65 years	29 (27.6)	
	≥ 65 years	76 (72.4)	
WHO Grade Group	Grade Group I (GS 6)	23 (21.9)	
	Grade Group II (GS 3+4)	11 (10.5)	
	Grade Group III (GS 4+3)	10 (9.5)	
	Grade Group IV (GS 8)	13 (12.4)	
	Grade Group V (GS 9-10)	48 (45.7)	
Arginase 2 Expression (Manual)	Score 0 (Negative)	8 (7.6)	
	Score 1 (Weak)	35 (33.3)	
	Score 2 (Moderate)	35 (33.3)	
	Score 3 (Strong)	27 (25.7)	
Arginase 2 Expression (H-Score)	Mean ± SD		124.65 ± 63.62
	Median (Min - Max)		135.00 (3.65 - 251.63)
TILs Density (%)	Mean ± SD		8.29 ± 10.96
	Median (Min - Max)		10.0 (0 - 50)
TILs Classification	Normal (0 - 9%)	51 (48.6)	
	Moderate (10 - 49%)	53 (50.5)	
	Severe (≥ 50%)	1 (0.9)	

Abbreviation: SD, Standard Deviation; GS, Gleason Score; TILs, Tumor-Infiltrating Lymphocytes.

Arginase 2 Down-regulation as a Marker of Dedifferentiation

A pivotal finding of this study is the significant inverse association between *ARG2* expression and the WHO Grade Group. We found that *ARG2* expression was highest in tumors that were well-differentiated (Grade Group I) and much lower in tumors that were poorly differentiated and high-grade (Grade Group V). This is in line with earlier biochemical research that found lower levels of arginase activity in the blood of men with high-grade prostate cancer [7, 16].

Androgen signaling is probably what caused this loss of expression. *ARG2* is a gene that responds to androgens [17]. As prostate cancer progresses, tumors frequently experience dedifferentiation and become independent of androgen signaling for growth maintenance. As a result, the expression of proteins regulated by androgens, such as *ARG2*, decreases. This phenomenon has been evidenced in vivo TRAMP models, wherein the depletion of *ARG2* correlated with a shift towards a more aggressive, neuroendocrine-like phenotype [18]. Our histopathological data indicate that persistent *ARG2* expression functions as a differentiation marker, whereas its absence denotes an aggressive tumor progression.

Prognostic Significance and Treatment Alternatives in ARG2-Negative Tumors

The downregulation or total loss of *ARG2* in high-

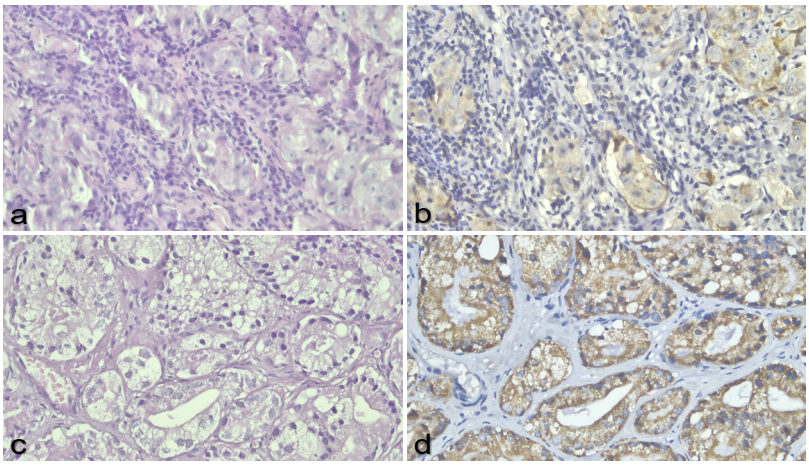

Figure 2. Inverse Spatial Correlation between Tumor-Infiltrating Lymphocytes (TILs) and *Arginase 2 (ARG2)* Expression. Dense stromal TIL infiltration on H&E (a) corresponds to weak *ARG2* expression on adjacent IHC (b). Conversely, tumor areas with minimal TILs (c) exhibit strong *ARG2* expression (d). (Magnification: 400x).

Table 2. Spearman Correlation Analysis between *Arginase 2* Expression (H-Score) and TILs Density under Various Analytical Scenarios

Analytical Scenario	Sample Group	n	Correlation Coefficient (r)	p-value
Global Analysis	Total Cohort	105	0.048	0.630
By Gleason Pattern	Dominant Pattern (Pattern 1)	105	0.016	0.869
	Secondary Pattern (Pattern 2)	97	-0.118	0.251
Sensitivity Analysis† (Excluding TILs 0%)	Dominant Pattern	54	-0.039	0.779
	Secondary Pattern	42	-0.171	0.303

†Sensitivity analysis was performed by excluding samples with 0% TILs to assess if the lack of correlation was driven by the high number of non-infiltrated tumors

grade prostate adenocarcinoma has considerable prognostic and therapeutic consequences. The absence of *ARG2* suggests tumor dedifferentiation and a possible transition to an androgen-independent or neuroendocrine-like phenotype, which typically signifies a worse clinical prognosis and accelerated disease progression [17, 18]. But this *ARG2*-negative state does have some unique weaknesses that can be used in therapy. Our spatial analysis shows that localized *ARG2* downregulation is linked to a higher TIL density. This is because these areas don't have the arginase-mediated "metabolic shield" that normally starves T-cells of L-arginine [12, 19]. Thus, prostate adenocarcinomas that are negative for or express low levels of *ARG2* may respond better to new immunotherapies, like immune checkpoint inhibitors (ICIs) [20], than those that are positive for *ARG2*. This is because they are in an immunologically "hotter" microenvironment. Moreover, since the loss of *ARG2* frequently coincides with the onset of castration-resistant prostate cancer (CRPC) [17], patients with significantly *ARG2*-downregulated tumors may derive diminished benefit from standard Androgen Deprivation Therapy (ADT) and may necessitate prompt evaluation for taxane-based chemotherapy, PARP inhibitors (in the context of homologous recombination repair mutations), or clinical trials aimed at dedifferentiated prostate cancer [21, 22].

The Paradox of Immune Infiltration: Global vs. Local Interactions

We found no statistical link between the overall *ARG2* H-Score and TILs density on a global level. This absence of correlation aligns with the comprehension that arginine metabolism within the tumor microenvironment (TME) is redundant and encompasses various enzymes, including Argininosuccinate Synthetase 1 (ASS1), indicating that *ARG2* alone does not govern systemic immune recruitment [23, 24].

Nonetheless, a contrasting scenario unfolded at the local microenvironmental level. Our spatial analysis demonstrated that tumor regions infiltrated by TILs showed markedly reduced *ARG2* expression in comparison to neighboring non-infiltrated regions. This is in line with the idea that spatial heterogeneity is a key part of the tumor microenvironment. Recent spatial profiling studies confirm this, showing that the microenvironment of prostate tumors is very compartmentalized, with unique immune and metabolic signatures that are often hidden in bulk tissue analysis [25]. Utilizing ecological principles in pathology indicates that the spatial distribution of immune cells rather than their total quantity is frequently more significant in influencing tumor progression and clinical results [26]. Two competing yet complementary hypotheses may elucidate this "immune exclusion" in high-*ARG2* regions [19]:

The Metabolic Shield Hypothesis

Elevated *ARG2* concentrations locally diminish extracellular L-arginine. T-cells need arginine to express the CD3ζ chain and move through the cell cycle. High-*ARG2* areas act like a "metabolic shield" that starves invading lymphocytes, making these areas an "immune desert" [12, 19, 27–29]. An analogous inverse correlation between metabolic enzyme expression and lymphocyte infiltration has been documented in other malignancies. For example, in endometrial cancer, elevated levels of Indoleamine 2,3-dioxygenase (IDO) an enzyme that breaks down tryptophan and works in a similar way to Arginase were strongly linked to fewer CD3+ and CD8+ tumor-infiltrating lymphocytes. This suggests that both enzymes work in the same way to keep immune cells from attacking tumors [30].

The Immunoediting Hypothesis

In contrast, recent findings indicate that *ARG2* may function as a tumor antigen identified by particular cytotoxic T-cells. It is conceivable that an active immune response has eradicated tumor clones exhibiting elevated *ARG2* expression in the infiltrated regions, resulting in the persistence of antigen-loss variants (low *ARG2*) that evade immune surveillance [31, 32]. This elucidates the predominance of TILs in regions characterized by low *ARG2* levels. This is in line with new ideas about cancer immunoediting and intratumor heterogeneity, which say that the adaptive immune system puts selective pressure on immunogenic subclones to get rid of them. As a result, the remaining tumor cells are immune-resistant variants that have lost certain antigens, such as *ARG2*, which lets them live in an environment full of immune cells [33].

Methodological Validation

The use of digital pathology makes these results more reliable. The high correlation ($r > 0.60$) between our digital H-Scores and manual pathological grading demonstrates that automated image analysis is an effective method for quantifying metabolic biomarkers in prostate tissue. This corroborates the increasing efficacy of digital pathology in reducing inter-observer variability, as indicated in recent literature [34–38].

Limitations

This study possesses limitations intrinsic to its design. H&E staining for TILs assessment does not facilitate the distinction between cytotoxic T-cells (CD8+) and regulatory T-cells (Tregs). This distinction is essential as *ARG2*-mediated arginine depletion can paradoxically facilitate Treg differentiation while suppressing effector T-cells [14]. Consequently, we are unable to ascertain whether the TILs identified in low-*ARG2* regions are functionally active anti-tumor cells or immunosuppressive Tregs. Future research employing multiplex immunohistochemistry is essential to accurately characterize these immune populations.

In conclusion, the expression of *Arginase 2* in prostate adenocarcinoma is markedly downregulated in high-grade tumors, indicating tumor dedifferentiation. *ARG2* does not universally predict immune infiltration; however, it has a localized impact on the tumor microenvironment (TME), where elevated expression is associated with immune exclusion. These results underscore *ARG2* as a prospective biomarker for tumor differentiation and a crucial metabolic regulator of local immunity.

Author Contribution Statement

Arif Budiman Kaharuddin: Conceptualization, data collection, formal analysis, and writing - original draft. Muhammad Husni Cangara: Supervision, methodology validation, and writing - review & editing. Upik Anderiani Miskad: Supervision, validation of histopathological grading, and critical review. Syarifuddin Wahid: Data curation and final approval of the version to be published. Djumadi Achmad: Resources provision and validation of immunohistochemical results. Berti Julian Nelwan: Investigation and clinical data correlation analysis.

Acknowledgements

General

The authors would like to express their sincere gratitude to the technical staff of the Anatomical Pathology Laboratory at Dr. Wahidin Sudirohusodo Hospital and Hasanuddin University Hospital for their excellent assistance in tissue processing and immunohistochemical staining. We also extend our appreciation to the archivists at Sentra Diagnostik Patologia Makassar for their support in retrieving the archival tissue blocks and clinical data used in this study.

Funding Statement

This research was self-funded by the authors and did not receive any specific grant from funding agencies in the public, commercial, or not-for-profit sectors.

Approval

This study is part of a thesis requirement for the Specialist Doctor Education Program in Anatomical Pathology and has been approved by the Department of Anatomical Pathology, Faculty of Medicine, Hasanuddin University.

Ethical Declaration

Ethical approval for this study was obtained from the Health Research Ethics Committee of the Faculty of Medicine, Hasanuddin University (Recommendation Number: [817A/UN4.6.4.5.31/PP36/2025).

Conflict of Interest

The authors declare that they have no competing interests regarding the publication of this paper.

References

1. Bray F, Laversanne M, Sung H, Ferlay J, Siegel RL, Soerjomataram I, et al. Global cancer statistics 2022: GLOBOCAN estimates of incidence and mortality worldwide for 36 cancers in 185 countries. CA Cancer J Clin. 2024;74(3):229–63. https://doi.org/10.3322/caac.21834
2. Yeole BB. Trends in the prostate cancer incidence in India. Asian Pac J Cancer Prev. 2008;9:141–4.
3. Safriadi F, Umbas R, Hakim L, Warli SM, Hamid AR, Hudaya S, Shidqy EM. Panduan penanganan kanker prostat. Ikatan Ahli Urologi Indonesia. 2022.
4. Smith GL, Lopez-Olivo MA, Advani PG, Ning MS, Geng Y, Giordano SH, et al. Financial Burdens of Cancer Treatment: A Systematic Review of Risk Factors and Outcomes. J Natl Compr Canc Netw. 2019;17:1184–92. https://doi.org/10.6004/jnccn.2019.7305
5. Memon A, Ahmad Z, Qureshi A, Ahsan A, Barakzai A, Bhurgri Y. Staging of prostatic adenocarcinoma with radical prostatectomy specimens in Pakistan. Asian Pac J Cancer Prev. 2009;10:551–4.
6. Sfanos KS, Yegnasubramanian S, Nelson WG, De Marzo AM. The inflammatory microenvironment and microbiome in prostate cancer development. Nat Rev Urol. 2018;15:11–24. https://doi.org/10.1038/nrurol.2017.167
7. Mumenthaler SM, Yu H, Tze S, Cederbaum SD, Pegg AE, Seligson DB, et al. Expression of arginase II in prostate cancer. Int J Oncol. 2008;32:357–65.
8. Hara M, Torisu K, Tomita K, Kawai Y, Tsuruya K, Nakano T, et al. *Arginase 2* is a mediator of ischemia–reperfusion injury in the kidney through regulation of nitrosative stress. Kidney Int. 2020;98:673–85. https://doi.org/10.1016/j.kint.2020.03.032
9. Niu F, Yu Y, Li Z, Ren Y, Li Z, Ye Q, et al. Arginase: An emerging and promising therapeutic target for cancer treatment. Biomed Pharmacother. 2022:149:112840. https://doi.org/10.1016/j.biopha.2022.112840
10. Li J, Zheng Y, Chen C, Lin Z, Pan J, Liang Y, et al. *Arginase 2* is a Diagnostic and Prognostic Marker for Prostate Cancer and Is Associated with Metabolism. Altern Ther Health Med. 2024;30(9):102–11.
11. Munder M. Arginase I is constitutively expressed in human granulocytes and participates in fungicidal activity. Blood. 2005;105(6):2549–56. https://doi.org/10.1182/blood-2004-07-2521
12. Grzywa TM, Sosnowska A, Matryba P, Rydzynska Z, Jasinski M, Nowis D, et al. Myeloid Cell-Derived Arginase in Cancer Immune Response. Front Immunol. 2020:11:938. https://doi.org/10.3389/fimmu.2020.00938
13. Bronte V, Zanovello P. Regulation of immune responses by L-arginine metabolism. Nat Rev Immunol. 2005;5(8):641–54. https://doi.org/10.1038/nri1668
14. Geiger R, Rieckmann JC, Wolf T, Basso C, Feng Y, Fuhrer T, et al. L-Arginine Modulates T Cell Metabolism and Enhances Survival and Anti-tumor Activity. Cell. 2016;167:829-842.e13. https://doi.org/10.1016/j.cell.2016.09.031

15. Hendry S, Salgado R, Gevaert T, Russell PA, John T, Thapa B, et al. Assessing Tumor-infiltrating Lymphocytes in Solid Tumors: A Practical Review for Pathologists and Proposal for a Standardized Method From the International Immunooncology Biomarkers Working Group: Part 1: Assessing the Host Immune Response, TILs in Invasive Breast Carcinoma and Ductal Carcinoma In Situ, Metastatic Tumor Deposits and Areas for Further Research. Adv Anat Pathol. 2017;24(5):235–51. https://doi.org/10.1097/PAP.0000000000000162
16. Elgün S, Keskineğe A, Yilmaz E, Baltaci S, Bedük Y. Evaluation of Serum Arginase Activity in Benign Prostatic Hypertrophy and Prostatic Cancer. Int Urol Nephrol. 1999;31:95–9. https://doi.org/10.1023/A:1007132109061
17. Gannon PO, Godin-Ethier J, Hassler M, Delvoye N, Aversa M, Poisson AO, et al. Androgen-regulated expression of arginase 1, *Arginase 2* and interleukin-8 in human prostate cancer. PLoS One. 2010;5(8):e12107. https://doi.org/10.1371/journal.pone.0012107
18. Mumenthaler SM, Rozengurt N, Livesay JC, Sabaghian A, Cederbaum SD, Grody WW. Disruption of arginase II alters prostate tumor formation in TRAMP mice. Prostate. 2008;68(14):1561–9. https://doi.org/10.1002/pros.20816
19. Chen DS, Mellman I. Elements of cancer immunity and the cancer–immune set point. Nature. 2017;541(7637):321–30. https://doi.org/10.1038/nature21349
20. Sharma P, Pachynski RK, Narayan V, Fléchon A, Gravis G, Galsky MD, et al. Nivolumab Plus Ipilimumab for Metastatic Castration-Resistant Prostate Cancer: Preliminary Analysis of Patients in the CheckMate 650 Trial. Cancer Cell. 2020;38(4):489-499.e3. https://doi.org/10.1016/j.ccell.2020.08.007
21. Cornford P, van den Bergh RCN, Briers E, Van den Broeck T, Brunckhorst O, Darraugh J, et al. EAU-EANM-ESTRO-ESUR-ISUP-SIOG Guidelines on Prostate Cancer—2024 Update. Part I: Screening, Diagnosis, and Local Treatment with Curative Intent. Eur Urol. 2024;86(2):148–63. https://doi.org/10.1016/j.eururo.2024.03.027
22. Mateo J, Carreira S, Sandhu S, Miranda S, Mossop H, Perez-Lopez R, et al. DNA-Repair Defects and Olaparib in Metastatic Prostate Cancer. N Engl J Med. 2015;373(18):1697-708. https://doi.org/10.1056/NEJMoa1506859
23. Hsueh EC, Knebel SM, Lo WH, Leung YC, Cheng PNM, Hsueh CT. Deprivation of arginine by recombinant human arginase in prostate cancer cells. J Hematol Oncol. 2012;5(1):17. https://doi.org/10.1186/1756-8722-5-17.
24. Matos A, Carvalho M, Bicho M, Ribeiro R. Arginine and arginases modulate metabolism, tumor microenvironment and prostate cancer progression. Nutrients. 2021;13(12):4503. https://doi.org/10.3390/nu13124503
25. Kumar V, Randhawa P, Bilodeau R, Mercola D, McClelland M, Agrawal A, et al. Spatial Profiling of the Prostate Cancer Tumor Microenvironment Reveals Multiple Differences in Gene Expression and Correlation with Recurrence Risk. Cancers (Basel). 2022;14(19):4923. https://doi.org/10.3390/cancers14194923
26. Yuan Y. Spatial Heterogeneity in the Tumor Microenvironment. Cold Spring Harb Perspect Med. 2016;6(8):a026583. https://doi.org/10.1101/cshperspect.a026583
27. Vilaça M, Correia Pinto J, Magalhães H, Reis F, Mesquita A. Tumor-Infiltrating Lymphocytes in Localized Prostate Cancer: Do They Play an Important Role? Cureus. 2023;15(1):e34007. https://doi.org/10.7759/cureus.34007
28. Taheri F, Ochoa JB, Faghiri Z, Culotta K, Park HJ, Lan MS, et al. l-Arginine Regulates the Expression of the T-Cell Receptor ζ Chain (CD3ζ) in Jurkat Cells1. Clin Cancer Res. 2001;7(3 Suppl):958s-965s.
29. Zea AH, Rodriguez PC, Culotta KS, Hernandez CP, DeSalvo J, Ochoa JB, et al. l-Arginine modulates CD3ζ expression and T cell function in activated human T lymphocytes. Cell Immunol. 2004;232(1-2):21–31. https://doi.org/10.1016/j.cellimm.2005.01.004
30. Ino K, Yamamoto E, Shibata K, Kajiyama H, Yoshida N, Terauchi M, et al. Inverse Correlation between Tumoral Indoleamine 2,3-Dioxygenase Expression and Tumor-Infiltrating Lymphocytes in Endometrial Cancer: Its Association with Disease Progression and Survival. Clin Cancer Res. 2008;14(8):2310-7. https://doi.org/10.1158/1078-0432.CCR-07-4144
31. Weis-Banke SE, Lisle TL, Perez-Penco M, Schina A, Hübbe ML, Siersbæk M, et al. Arginase-2-specific cytotoxic T cells specifically recognize functional regulatory T cells. J Immunother Cancer. 2022;10(10):e005326. https://doi.org/10.1136/jitc-2022-005326
32. Líndez AAM, Dunand-Sauthier I, Conti M, Gobet F, Núñez N, Hannich JT, et al. Mitochondrial arginase-2 is a cell autonomous regulator of CD8+ T cell function and antitumor efficacy. JCI Insight. 2019;4(24):e132975. https://doi.org/10.1172/jci.insight.132975
33. Roerden M, Spranger S. Cancer immune evasion, immunoediting and intratumour heterogeneity. Nat Rev Immunol. 2025;25(5):353–69. https://doi.org/10.1038/s41577-024-01111-8
34. Bankhead P, Loughrey MB, Fernández JA, Dombrowski Y, McArt DG, Dunne PD, et al. QuPath: Open source software for digital pathology image analysis. Sci Rep. 2017;7(1):16878. https://doi.org/10.1038/s41598-017-17204-5
35. Morriss NJ, Conley GM, Ospina SM, Meehan WP, Qiu J, Mannix R. Automated Quantification of Immunohistochemical Staining of Large Animal Brain Tissue Using QuPath Software. Neuroscience. 2020;429:235–44. https://doi.org/10.1016/j.neuroscience.2020.01.006
36. Omura A, Kimura T, Maniwa T, Watabe T, Honma K, Shintani Y, et al. Quantification of the immunohistochemical staining of fibroblast activation protein in intrathoracic solitary fibrous tumors using QuPath. Surg Today. 2025;55(9):1269–73. https://doi.org/10.1007/s00595-025-03024-y
37. Loughrey MB, Bankhead P, Coleman HG, Hagan RS, Craig S, McCorry AMB, et al. Validation of the systematic scoring of immunohistochemically stained tumour tissue microarrays using QuPath digital image analysis. Histopathology. 2018;73(2):327–38. https://doi.org/10.1111/his.13516
38. Qureshi A, Lakhtakia R, AL Bahri M, Al Haddabi I, Saparamadu A, Shalaby A, et al. Gleason's Grading of Prostatic Adenocarcinoma: Inter-Observer Variation Among Seven Pathologists at a Tertiary Care Center in Oman. Asian Pac J Cancer Prev. 2016;17(11):4867–8. https://doi.org/10.22034/APJCP.2016.17.11.4867